日本医放会誌：52（3），261—267，1992（平4）

＜特別講演＞
第50回総会（1991年4月）

Radiologico-Pathological Correlation in MR Imaging

Man Chung Han
Department of Diagnostic Radiology, Seoul National University College of Medicine, Seoul, Korea

Research Code No. : 500.9

Key Words : MR, MR comparative studies, MR experimental

Magnetic resonance (MR) imaging was first introduced in 1972 and it became clinically applicable in 1981. Since then, there has been a great explosion of interest in MR and the routine use of MR imaging is becoming a reality in the United States and Western Europe. The clinical use of MR is also becoming widespread in Japan and Korea[1].

Seoul National University Hospital has two MR imaging units; one is a 2.0 T superconductive magnet (Spectro-20000; Goldstar, Seoul) and the other is a 0.5 T superconductive one (Supertec-5000; Goldstar, Seoul), which were set up in 1988 and 1989, respectively. Up until February 1991, a total of 13,880 cases of MR imaging, mostly brain, head and neck, and spine, have been performed (Table 1).

MR imaging has distinct advantages over other imaging modalities, namely its superb soft-tissue contrast resolution and multiplanar imaging capability. Thanks to these advantages, MR imaging has a great potential in demonstrating detailed sectional human anatomy[2], in characterizing pathologic processes and in evaluating the extent of local tumor spread. The purpose of this communication is to present and discuss some selected data which will serve as a ground for the answers to the following two questions; 1) How MR imaging findings correlate with macroscopic or microscopic findings? 2) What are the pathologic bases of MR imaging findings in various disease states?

MR is now accepted as the essential imaging modality in the evaluation of the brain and spinal cord, as well as the head and neck[3)~8)]. It has been proposed that hemorrhage can be uniquely characterized on

Table 1 Organ Distribution of MR Examinations

Examination organ	Case No.(%)
Brain	7,545(54.4)
Sella	428(3.1)
Head and Neck	116(0.8)
Spine	3,511(25.3)
Musculoskeletal system	884(6.4)
Abdomen	430(3.1)
Pelvis	413(3.0)
Chest	115(0.8)
Cardiovascular system	169(1.2)
Others	269(1.9)
Total	13,880(100)

(Seoul National University Hospital, May 1988-February 1991)

平成4年3月25日

high-field MR images on the basis of magnetic susceptibility variations of the sequential degradation products of hemoglobin in an evolving hemorrhage[9]. Consequently, MR imaging is considered to be sensitive in detecting and characterizing hemorrhagic processes of the brain. In brain tumors containing hemorrhagic components such as cavernous hemangioma, glioblastoma multiforme, or metastatic tumors, MR imaging is superior to CT in elucidating tumor components leading to a more accurate preoperative diagnosis. In these hemorrhagic tumors, MR imaging shows marked signal heterogeneity representing a viable tumor component and various evolving stages of hemorrhage.

To evaluate the MR appearances of an acute intracerebral hemorrhage (ICH) both at 2.0 T and 0.5 T field strength, MR imaging was performed in 15 cats after an experimental acute ICH was produced by injecting 1.5 ml of autologous femoral arterial blood into the parietal lobe. Findings of MR images were well correlated with their pathologic counterparts with regard to extent and nature of acute ICH at both 2.0 T and 0.5 T. However, MR images at 2.0 T appeared superior to those at 0.5 T. Immediately following the inoculation of the hematoma, the signal intensity of the hematoma was isointense or slightly hypointense in all spin-echo pulse sequences and markedly hypointense in gradient-echo sequences. In hematomas older

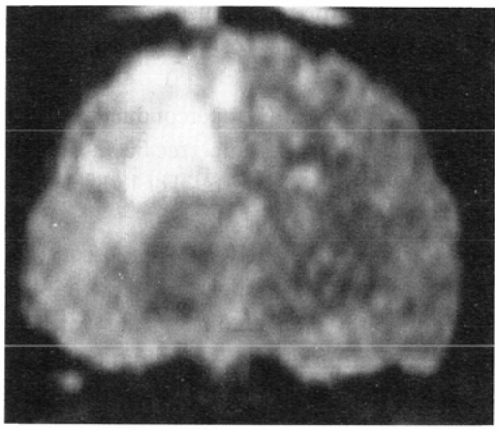

(a)

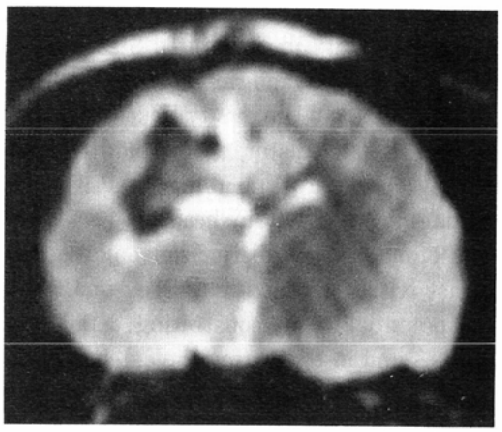

(b)

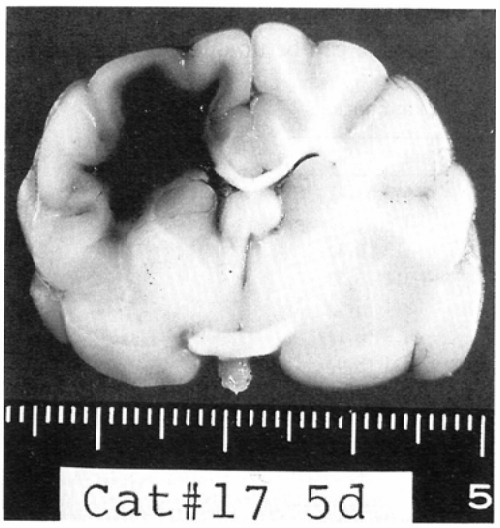

(c)

Fig. 1 Coronal images of 5-day-old experimentally produced intracerebral hematoma in cat.
(a) T2-weighted image at 0.5 T shows high signal intensity of the lesion.
(b) T2-weighted image at 2.0 T shows low signal intensity of the lesion and peripheral edema of high signal intensity.
(c) Photograph of a cut-surface of the specimen.

than 6 hours following the inoculation, the signal intensity was hypointense at 2.0 T, but hyperintense at 0.5 T (Fig. 1). On gradient-echo images, hematomas older than 6 hours had marked hypointensity and appeared larger than those on spin-echo images. Routine spin-echo pulse sequences were adequate for the detection of acute ICH at 2.0 T, but not at 0.5 T. Gradient-echo technique was useful as a complementary sequence in the evaluation of acute ICH, particularly at 0.5 T[10].

The composition of tumor and the degree of its cellularity have an effect in tumor signal intensity on T1- and T2-weighted images. On T2-weighted images in general, a tumor with compact, high cellularity shows a relatively low signal intensity, and a tumor with sparse, low cellularity and abundant interstitial fluid shows a relatively high signal intensity (Fig. 2, 3). Therefore, such MR signal characteristics could be used reliably to predict pathologic subtypes of meningiomas[11].

MR imaging has had a significant impact on the musculoskeletal radiology, the oldest subspecialty of radiology, primarily owing to its excellent spatial and contrast resolution. We performed a study of MR imaging-pathology correlation of avascular necrosis of the femoral head. The low signal intensity surrounding the lesion was mainly due to bony sclerosis. The resorbed reactive fibrous areas showed a relatively high signal intensity, necrotic debris with or without dystrophic calcifications showed a low signal intensity, and finally the cartilage, either articular or callous, showed a low signal intensity[12]. Although MR images, as in other radiographs, may be negative for a period of time before characteristic changes of avascular necrosis can be visualized, MR imaging will be a noninvasive means of diagnosing avascular necrosis in its early stage.

MR imaging is widely considered to be reliable in staging musculoskeletal tumors, in that limited or limb-saving surgery in patients with primary malignant bone tumors is becoming possible. An experimental high-field MR imaging of VX-2 carcinoma inoclulated at the thigh muscles of 28 rabbits disclosed that MR imaging could differentiate not only the viable tumor from necrotic tissues but also the different stages of the tumor necrosis. Detectability of necrotic portions of the tumor was the highest by T1-weighted images with contrast enhancement followed by T2-weighted images, proton density images,

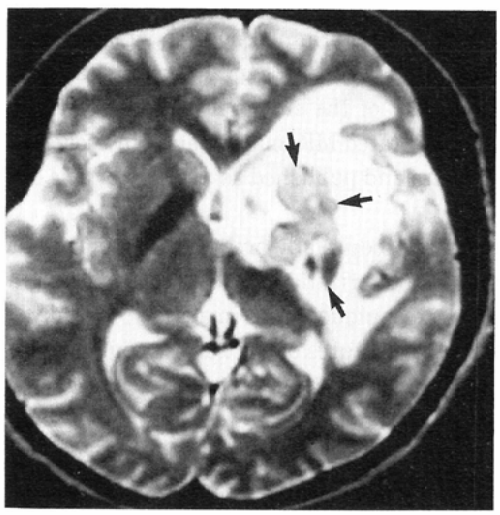

(a)

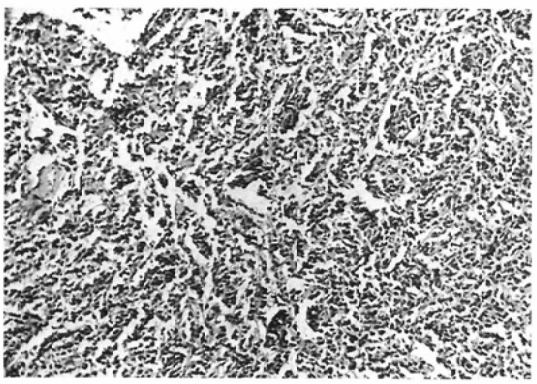

(b)

Fig. 2 A 30-year-old female with lymphoma of the brain.
(a) T2-weighted image shows tumor mass of intermediate signal intensity (arrows) and surrounding edema of high signal intensity.
(b) Photomicrograph of the specimen shows compact cellularity of the tumor.

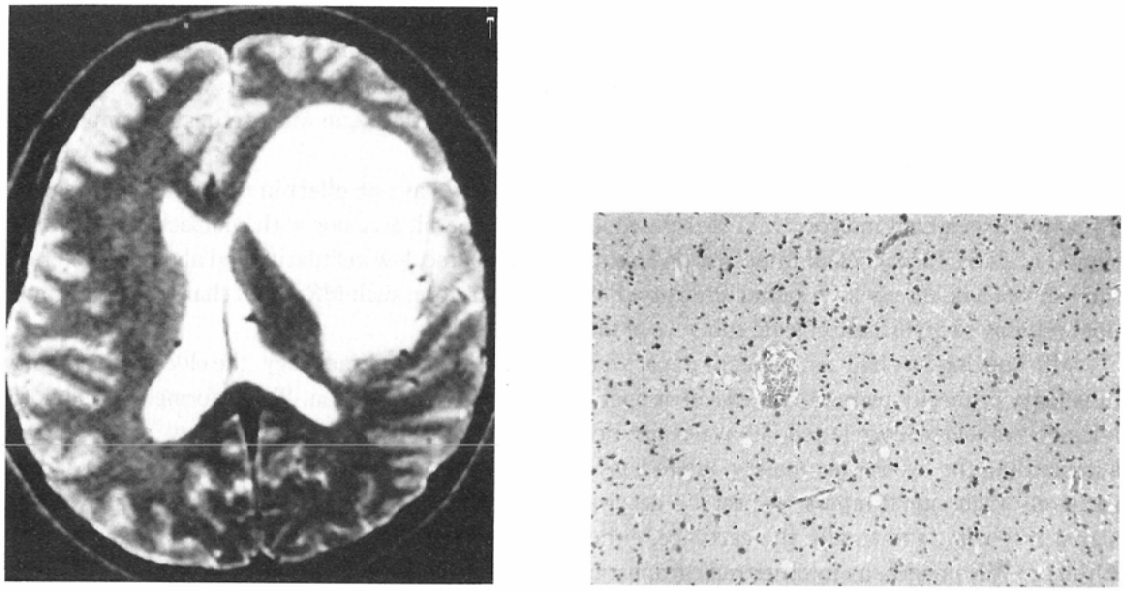

(a) (b)

Fig. 3 A 23-year-old female with low grade astrocytoma.
(a) T2-weighted image shows high signal intensity of the tumor.
(b) Photomicrograph of the specimen shows low cellularity of the tumor.

and T1-weighted images. However, T2-weighted images were the best in evaluating the nature of necrotic tissues. On T2-weighted images, low intensity areas corresponded to the areas of early stage of necrosis, iso-intensity areas corresponded to the areas of intermediate stage of necrosis, and high intensity areas corresponded to the areas of late stage of necrosis[13]. The other experimental MR imaging study using 17 rabbits with VX-2 carcinoma revealed that the extent of the lesion determined by high signal intensity areas was larger than the true extent of the tumor evaluated by pathological examination. This phenomenon was presumably caused by the high signal intensity of the surrounding loose connective tissue rich in blood vessels and lymphatics[14]. A meticulously illustrated MR imaging-anatomy correlation has been successfully performed using various joints of cadavers and published as an atlas by one of my colleagues in our department[15].

Although MR imaging of the abdomen is marred by artifacts produced by breathing movements, MR imaging has yielded promising results for the detection and characterization of abdominal masses, and further progress is expected with the use of rapid scanning techniques. MR imaging, especially T2-weighted images, could demonstrate the internal morphologic architectures of the hepatic tumors[16]. In an encapsulated hepatocellular carcinoma, the capsule showed low intensity relative to the liver parenchyma on both T1- and T2-weighted images, and viable tumor nodules showed low intensity on T1-weighted images and high intensity on T2-weighted images. The areas of coagulation necrosis without hemorrhage showed low intensity on both T1- and T2-weighted images, but those with hemorrhagic component showed heterogeneous high signal intensity on both pulse sequences[17]. The interpretation of the MR images of the hepatocellular carcinoma following chemoembolization using Lipiodol should be done carefully since the signal intensity of the lesion may be affected by the embolization with contrast material[18,19]. Further study will be necessary in this regard.

MR imaging supplanted the other imaging modalities in characterizing focal hepatic lesions,

particularly in differentiating hemangiomas from hepatocellular carcinomas. Using our 2.0 T magnet, spin-echo 2000/60 [TR/TE, msec] sequence was optimal for the detection of small hepatocellular carcinomas and hemangiomas, and spin-echo 2000/150 sequence was optimal for distinguishing small hepatocellular carcinomas from hemangiomas[20]. In a case of retroperitoneal teratoma, five main components of the tumor—bone, solid adipose tissue, sebum and hair, and loose edematous fibrofatty tissue with skin— could be differentiated from one another on the basis of signal intensities on various pulse sequences[21].

There are still vast regions to be explored in the field of renal imaging. The results of early investigations suggested that MR imaging would prove valuable in the assessment of renal diseases. Although the obliteration of corticomedullary contrast on T1-weighted MR images is a nonspecific finding, there are some reports suggesting specific MR imaging findings in certain renal diseases[22,23]. In patients with a severe form of hemorrhagic fever with renal syndrome, MR imaging of the kidney has clearly and consistently demonstrated the low signal intensity along the outer medulla on T2-weighted images, probably representing medullary hemorrhage containing intracellular deoxyhemoglobin or intracellular methemoglobin[22]. MR imaging finding of very low signal intensity in the renal cortex on both T1- and T2-weighted images is also very specific for disorders of chronic hemolysis such as paroxysmal nocturnal hemoglobinuria or sickle cell nephropathy[23].

We performed experimental MR imaging studies following renal artery and vein ligation using 38 rabbits, simulating renal artery embolism and renal vein thrombosis, respectively[24,25]. In the study of renal artery ligation, the signal intensity of the renal medulla decreased both on T1- and T2-weighted images up to 24 hours after the ligation. This MR imaging findings could be explained by histopathologic changes of complete arterial occlusion i.e., diminished perfusion, congestion and interstitial hemorrhage in the renal medulla[24]. Following the ligation of renal vein, kidney was enlarged and corticomedullary contrast was obliterated on T1-weighted images. On T2-weighted images, there were low signal intensities along the outer medulla and subcapsular cortex. MR imaging-pathologic correlation revealed that the inner low signal intensity zone was matched with congestion and hemorrhage at the outer medulla and the peripheral rim of low signal intensity represented subcapsular hemorrhage and congestion within the subcapsular cortex.

MR imaging provides an accurate assessment of the female genital organs and related diseases. In a comparative study on CT and MR imaging with pathologic correlation in uterine cervical carcinomas, MR imaging was far more superior to clinical evaluation and CT in detecting parametrial invasion and in staging uterine cervical carcinomas[26]. MR imaging also provides an information about the depth of tumor invasion of cervical stroma. At this point, we recommend MR imaging in lieu of CT as a routine imaging study for preoperative staging of uterine cervical carcinomas.

To date, MR imaging lags behind thin-slice CT in the evaluation of lung parenchyma. However, MR imaging was found to be comparable with thin-slice CT for delineating normal anatomic structures of cadaver lung specimens. It is anticipated that with further technical modifications, the role of MR imaging as a clinical tool to evaluate the lung may expand. MR imaging also has a potential role in the evaluation of extent and nature of mediastinal lesions, and possibly in the differentiation of active and inactive lymph nodes involved in disease processes such as tuberculosis. MR imaging is particularly useful in demonstrating vascular structures within tumor masses in that more detailed information about tumor characteristic can be obtained.

Cardiac MR imaging is helpful in the diagnosis of congenital and acquired heart diseases because it delineates the cardiac chambers accurately. In patients with mitral stenosis spin echo MR imaging is believed to be a valuable diagnostic modality that provides pathoanatomical and physiological informa-

tion[27]. MR imaging, especially gradient-echo imaging, is also useful in the evaluation of extent and nature of thrombi in the heart, great vessels, and deep veins of the extremities.

In conclusion, MR imaging is the most promising modality in terms of radiologico-pathological correlation among various imaging methods available to day and it is indispensable for radiologists to understand the pathological basis of MR imaging with further investigation and clinical application.

References

1) Han MC, Lee JS, Chung JW, et al: An analysis on initial 2084 cases of magnetic resonance imaging. J Korean Radiological Society 25: 162—167, 1989
2) Han MC, Kim CW: Sectional human anatomy correlated with CT and MRI. 2nd ed. 1989, Ilchokak, Seoul, Korea
3) Chang KH, Han MH, Choi YW, et al: Tuberculous arachnoiditis of the spine: Findings on myelography, CT and MR imaging. AJNR 10: 1255—1262, 1989
4) Suh DC, Chang KH, Han MH, et al: Unusual MR manifestations of neurocysticercosis. Neuroradiol 31: 396—402, 1990
5) Chang KH, Han MH, Roh JK, et al: Gd-DTPA enhanced MR imaging in intracranial tuberculosis. Neuroradiol 32: 19—25, 1990
6) Chang KH, Yi JG, Han MH, et al: Clinical utility of partial flip angle T2-weighted spin-echo imaging of the brain. Neuroradiol 32: 255—260, 1990
7) Chang KH, Han MH, Roh JK, et al: Gd-DTPA-enhanced MR imaging of the brain in patients with meningitis: comparison with CT. AJR 154: 809—816, 1990
8) Han MH, Chang KH, Lee CH, et al: Sinonasal psammomatoid ossifying fibromas: CT and MR manifestations. AJNR 12: 25—30, 1991
9) Gomori JM, Grossman RI: Mechanisms responsible for the MR appearance and evolution of intracranial hemorrhage. RadioGraphics 8: 427—440, 1988
10) Lee MG, Chang KH, Han MH, et al: An experimental study on MR imaging of acute intracerebral hematoma: Comparative analysis between high-field (2.0 T) and medium-field (0.5 T) images. J Korean Radiological Society 27: 5—14, 1991
11) Elster AD, Challa VR, Gilbert TH, et al: Meningiomas: MR and histopathologic features. Radiology 170: 857—862, 1989
12) Kang HS, Lee SH, Lee YS, et al: MR microscopy of avascular necrosis of femur head. Presented at the 5th Asian-Oceanian Congress of Radiology. September 21—25, 1987
13) Choi BI, Lee DH, Suh JW, et al: Tumor portions and necrotic portions of VX-2 carcinoma in rabbits: Correlation with MRI and pathology. J Korean Radiological Society 26: 230—241, 1990
14) Chung SH, Kang HS, Han MC, et al: An experimental study on evaluation of MR imaging in determining the extent of the VX-2 carcinoma of rabbits. (unpublished data)
15) Kang HS, Resnick D: MRI of the extremities: An anatomic atlas. 1991, W.B. Saunders, Philadelphia
16) Choi BI, Han MC, Park JH, et al: Giant cavernous hemangioma of the liver: CT and MR imaging in 10 cases. AJR 152: 1221—1226, 1989
17) Choi BI, Lee GK, Kim ST, et al: Mosaic pattern of encapsulated hepatocellular carcinoma: Correlation of magnetic resonance imaging and pathology. Gastrointest Radiol 15: 238—240, 1990
18) Yoshioka H, Nakagawa K, Shindou H, et al: MR imaging of the liver before and after transcatheter hepatic chemo-embolization for hepatocellular carcinoma. Acta Radiol 31: 63—67, 1990
19) Buckwalter KA, Ellis JH, Baker DE, Borello JA, Glazer GM: Pitfall in MR imaging of lymphadenopathy after lymphangiography. Radiology 161: 831—832, 1986
20) Choi BI, Han MC, Kim CW: Small hepatocellular carcinoma versus small cavernous hemangioma: Differentiation with MR imaging at 2.0 T. Radiology 176: 103—106, 1990
21) Choi BI, Chi JG, Kim SH, et al: MR imaging of retroperitoneal teratoma: Correlation with CT and pathology. J Comput Assist Tomogr 13: 1083—1086, 1989
22) Kim SH, Kim S, Lee JS, et al: Hemorrhagic fever with renal syndrome: MR imaging of the kidney. Radiology 175: 823—825, 1990
23) Kim SH, Han JS, Lee JS, et al: Paroxysmal nocturnal hemoglobinuria: Case report of MR imaging and CT findings. Acta Radiol 32: 315—316, 1991

24) Suh CH, Kim CW, Han MC, et al: Magnetic resonance imaging of renal ischemia experimentally induced by renal artery ligation. (unpublished data)
25) Byun HS, Kim CW, Han MC, et al: Magnetic resonance imaging of rabbit kidney after renal vein ligation. (unpublished data)
26) Kim SH, Choi BI, Lee HP, et al: Uterine cervical carcinoma: Comparison of CT and MR findings. Radiology 175: 45—51, 1990
27) Park JH, Han MC, Oh BH, et al: Magnetic resonance evaluation of mitral stenosis. Cardiovasc Intervent Radiol 13: 294—299, 1990